FEBS Letters 587 (2013) 2517–2522

journal homepage: www.FEBSLetters.org

Biochemical evidence of key residues for the activation and autoprocessing of tomato type II metacaspase

Shuai Wen [1], Qiu-Min Ma [1], Ya-Li Zhang, Ji-Ping Yang, Guang-Hua Zhao, Da-Qi Fu, Yun-Bo Luo, Gui-Qin Qu *

College of Food Science and Nutritional Engineering, China Agricultural University, No. 17 Qinghua East Road, Beijing 100083, China

ARTICLE INFO

Article history:
Received 4 June 2013
Revised 28 June 2013
Accepted 28 June 2013
Available online 11 July 2013

Edited by Ulf-Ingo Flügge

Keywords:
Tomato
Metacaspase
Autoprocessing
Activation
Site-directed mutagenesis

ABSTRACT

To investigate the autolysis pattern and activation of metacaspase in higher plants, the biochemical characteristics of purified recombinant type II metacaspase (LeMCA1) from tomato were explored. Western blotting analysis indicated that four cleaved bands were formed; two N-terminal fragments and two C-terminal fragments. N-terminal sequencing confirmed that LeMCA1 cleaves at Lys223 and Arg332. Site mutants indicated that catalytic Cys139, cleaved Lys223, Arg332 and predicted calcium binding Asp116/Asp117 are the key residues that are responsible for its Ca^{2+} and pH dependent activation. The cleavage of the full-size fragment seemed crucial for the activation of LeMCA1 in vitro.

Structured summary of protein interactions:
LeMCA1 and **LeMCA1** cleave by enzymatic study (View Interaction: 1, 2).

1. Introduction

Metacaspase belongs to the clan CD cysteine proteases that shares a core protein fold containing the catalytic His/Cys dyad, similar to that found in caspases [1]. They can be divided into type I and type II groups based on their sequence similarity and domain structure [2]. Both types contain two domains predicted to relate to the p20 and p10 subunits of animal caspases but differ in that only type I has a predicted N-terminal prodomain, whereas type II harbor a linker region between the subunits [3]. Metacaspases are found in plants, fungi and protozoa but absent in metazoan [2]. In plants, metacaspases have been identified as a primary positive regulator in oxidative stress and pathogen induced programmed cell death [4–8], and are also essential for Norway Spruce embryogenesis [9]. In yeast and some protozoa, metacaspases are involved in protein aggregation, ER stress and cell proliferation [3,10–12].

Compared with caspases, metacaspases, both from plant and lower organisms, can be autocatalytically processed when overproduced in bacterial cells, which leads to the appearance of different size polypeptides [13]. N-terminal sequencing has identified that cleavage events occur at arginine (R) or lysine (K) residues in plants (R183 in AtMC9, K225 in AtMC4, R188 and K269 in Norway spruce [9,14,15]). Nonetheless, a number of cleavage sites remain unresolved and the proteolytic patterns appear to be more complex in higher dicotyledonous plants. Ca^{2+} stimulates metacaspase autolysis in vitro and metacaspase activity also exhibits a Ca^{2+}-dependence [13,14]. However, the mechanism and relationship between Ca^{2+} and autolysis remains unclear and debatable. Identification of multiple self-processing sites and the use of site-directed mutagenesis to dissect the functional relevance of these cleavage sites in different species should allow us to provide more information to analysis the autolysis biochemical function in higher plant.

The tomato is one of the most widely studied model plants in development regulation and stress response, due to its relatively small genome and well-characterized mutant lines [16]. The tomato type II metacaspase (LeMCA1) gene is located in tomato chromosome 9, which was unregulated during programmed cell death in *Botrytis cinerea*-infected leaves [7]. Here, we have analyzed the biochemical autolysis pattern and the factors that affect the activation of recombinant LeMCA1. Mutants with different cleavage sites were then used to identify which particular residues affect the autoprocessing and activities of LeMCA1. The results will

Abbreviations: LeMCA1, tomato metacaspase; AtMC1–9, *Arabidopsis* metacaspase 1–9; TaMCA4, wheat metacaspase 4; MCA2, *Trypanosoma brucei* metacaspase 2; mcII-Pa, Norway spruce metacaspase; Yca1, Yeast metacaspase; GRR, Boc-Gly-Arg-Arg-MCA

* Corresponding author. Fax: +86 10 62737465.
E-mail addresses: guguiqin2000@sina.com, 897122103@qq.com (G.-Q. Qu).

[1] These authors contributed equally to this work.

0014-5793/$36.00
http://dx.doi.org/10.1016/j.febslet.2013.06.057

aid our understanding of the biochemical structure and function of MCAs in higher plant systems.

2. Materials and methods

2.1. Production of LeMCA1 recombinant protein

The LeMCA1 coding sequence was amplified from *Lycopersicon esculentum* leaves cDNA with forward and reverse primers 5′-GAATTCATGGCGAAAAAAGC-3′ and 5′-CTCGAGACAAACAAAAG-GAGCATC-3′. The cDNA product was inserted into the restriction sites E*coRI* and X*hoI* of the pET28a (Novagen) vector, leading to a His-tag located at both the N- and C-termini. Plasmid encoding LeMCA1 was transformed into BL21 (DE3) pLysS *Escherichia coli* competent cells (Transgen). Protein expression was induced by the addition of isopropyl-β-D-thiogalactopyranoside to a final concentration of 1 mM. The culture was grown for a further 3 h at 37 °C with an $A_{600}$of 0.6. Bacteria were disrupted by sonication in extraction buffer [9]. The supernatant, after centrifugation to remove cell debris, was applied to a Ni-column (GE Health) for protein purification. Ten, 20 and 250 mM imidazole were used as binding, washing and elution buffers, respectively.

2.2. Site-directed mutation

Five mutant forms of LeMCA1 (LeMCA1^{C139A}, LeMCA1$^{R186A/K269A}$, LeMCA1^{k223G}, LeMCA1^{R332A} and LeMCA1$^{D116A/D117A}$ were constructed by the GenScript Corporation (Nanjing, China). Mutants were confirmed by DNA sequencing analysis.

2.3. Enzyme activity assays

LeMCA activity was measured by incubation of ~5 μg purified protein for 0–30 min at 28 °C with 50 μM fluorescent substrate Boc-GRR-MCA (Peptide institute) in a 100 μL reaction buffer (100 mMHepes (pH 7.0), 0.1% CHAPS, 5 mM dithiothreitol) with 50 mM $CaCl_2$, unless otherwise stated [9]. Assay buffers of varying pH were prepared as follows: pH 4–5, 50 mM NaAc; pH 5.5–6.5, 50 mM MES; pH 7–8, 100 mM Hepes; pH 8.5–9, 100 mM Tris. The proteolytic activities were measured using a multifunctional fluorescence reader (Tecan), with excitation at 368 nm and emission at 465 nm. All experiments were run in triplicate.

2.4. SDS–PAGE and immunoblotting analysis

Proteins were separated by 12% (v/v) SDS–PAGE. Separated proteins were electrophoretically transferred to a NC membrane (0.45 μm, Invitrogen). After blocking, the membrane was probed with the monoclonal anti-T7 antibody (1:5000; Novagen), the monoclonal anti-HIS antibody (1:5000; Invitrogen), or the polyclonal anti-LeMCA1 antibody (1:5000, our lab) at room temperature for 1 h. LeMCA1 polyclonal antiserum was obtained from immunized mice. Goat anti-mouse IgG conjugated with horseradish peroxidase (1:10 000, Dako) was used as the secondary antibody.

2.5. N-terminal peptide sequencing of LeMCA1 fragments

Purified LeMCA1 separated by SDS–PAGE analysis was transferred to a PVDF membrane (0.45 μm, Millipore). After staining the membrane with Coomassie Brilliant Blue, the membrane was submitted to the college of Life Sciences, Peking University for Edman sequencing.

2.6. Homology modeling to predict the three-dimensional structure

Based on the PSI-BLAST in NCBI database (http://blast.ncbi.nlm.nih.gov/Blast.cgi) and Fold Prediction Metaserver (https://genesilico.pl/), the bacterial caspase-like protein GSU0716 from *Geobacter sulfurreducens* and its crystal structure (PDB 3BIJ) were chosen as the most appropriate template for homology modeling of LeMCA1. Three-dimensional structure models were constructed by Modeller 9.11 with combined Python 2.7 in automode and details were modified manually through SPDB Viewer 4.1.0. Online MetaMQAP Serve were applied to assess the homology modeling results using the algorithm and methods in the server.

3. Results

3.1. Sequence and structure characteristics of tomato LeMCA1

Based on the tomato metacaspase partial cDNA sequence (AY114141), we designed primers and obtained the coding region of LeMCA1 (GenBank Deposition No.: JX839683). The coding region shares between 71% and 78% amino acid similarity with plant type II metacaspase of Arabidopsis (AtMC4 to AtMC7), Norway spruce (mcII-*Pa*) and Wheat (TaMCA4); however, a lower sequence similarity range between 28% and 37% was observed with protozoa *Trypanosomabrucei* MCA2, Yeast Yca1 and other plant type I metacaspases (Fig. S1). H86 and C139 are conserved catalytic residues of LeMCA1, which is the same as other metacaspases (Fig. S2). Phylogenetic analysis revealed that LeMCA1 is the closest relative of TaMCA4 and mcII-Pa type II metacaspases and has a common ancestor with all *A. thaliana* type II metacaspases (Fig. S3). According to the sequence blastand phylogenetic analysis results, LeMCA1 had closer identity to AtMC4–9, mcII-Pa and TaMCA4.

3.2. Purified recombinant LeMCA1 shows calcium and pH-dependent activation

To describe the biochemical characteristics of recombinant tomato LeMCA1 in vitro, we first identified purified LeMCA1 by Western blot analysis using a LeMCA1 antibody (data not shown). Fluorogenic Boc-GRR-MCA substrates were then used to detect the effects of ion, pH and temperature on the activity of LeMCA1 [3]. Fig. 1A shows that the presence of Ca^{2+} noticeably increases the activity of LeMCA1 in a dose dependent manner. The accelerated hydrolysis rate of Boc-GRR-MCA was observed in Ca^{2+} concentrations >10 mM. The presence of the calcium chelating agent EDTA completely abolished the activity of LeMCA1 (Fig. 1B). Other ions such as K^+, Na^+, Zn^{2+} and Mg^{2+} had no significant enhancement on the activity of LeMCA1 (data not shown). LeMCA1 was found to have a pH optimum between 7.0 and 7.5 as shown in Fig. 1C. pH values lower than 5 or higher than 9 resulted in the complete loss of activities.

To detect whether temperature affects the LeMCA1 GRR activity, enzymatic reactions were carried out at 4, 28, 37 and 42 °C with optimal Ca^{2+} (50 mM) and pH conditions (7.5). Fig. 1D shows that the GRR activities at 4, 37 and 42 °C are slightly lower than that at 28 °C, but there was no distinct difference in activity. This observation suggests that LeMCA1 functions over a wide temperature range.

3.3. Auto-proteolysis pattern of recombinant LeMCA1

Both type I and type II metacaspases exhibit auto-proteolysis when they are over-expressed in bacteria [9,13,14]. In our research system, purified LeMCA1 also showed several bands identified by anti-LeMCA1, including a 60 kDa full-length protein, as well as ~38, 32, 26 and 18 kDa fragments (Fig. 2A). An immunoblot with anti-T7 or anti-His further confirmed that the ~38 and ~32 kDa bands are the processing forms of the N-terminal with T7 tag, whereas the other two fragments are the C-terminal processing bands (Fig. 2A). These data suggest that autoprocessing occurred at multiple sites of purified LeMCA1.

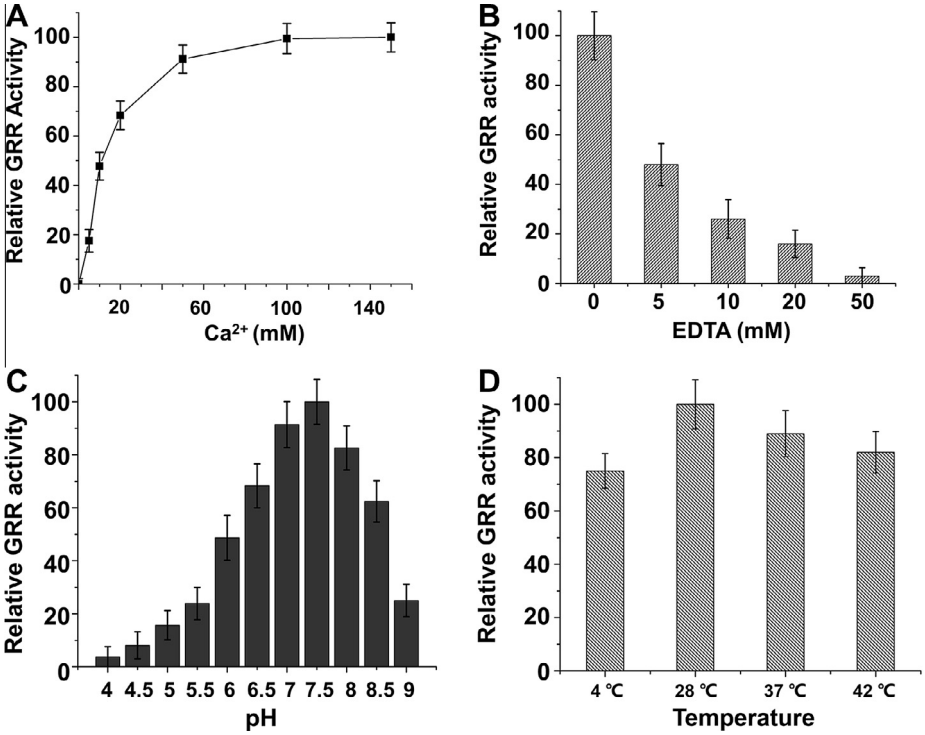

Fig. 1. Effect of ion, pH and temperature on the GRR activity of LeMCA1. (A) Ca^{2+}-dependent activation profile of GRR activity. (B) Inhibition of GRR activity by indicated concentration of EDTA with 50 mM Ca^{2+}. (C) The GRR activity at different pH with 50 mM Ca^{2+}. (D) The GRR activity of LeMCA1 at 4, 28, 37 and 42 °C with 50 mM Ca^{2+} and pH 7.5. Enzyme activity assays system containing 5 μg LeMCA1 proteins and 50 μM GRR-MCA.

To map the auto-proteolysis sites of LeMCA1, we selected the ~26 and 18 kDa bands for N-terminal sequencing. After analyzing the sequencing, K223 and R332 were identified as the auto-proteolysis sites of LeMCA1 (Fig. 2B). These results provide direct evidence that LeMCA1 has specially cleavage sites at K223 and R332.

Ca^{2+} and pH affected the activities of purified LeMCA1 (see Fig. 1C). To identify whether Ca^{2+} and pH have an effect on the autoprocessing pattern of LeMCA1, purified LeMCA1 was first incubated with or without 50 mM $CaCl_2$ for 3, 6, 9, 12, 15 and 18 min at 28 °C and analyzed by SDS–PAGE. Fig. 3A shows that full-length LeMCA1 as well as ~38 kDa fragments are more rapidly degraded in 50 mM Ca^{2+} than in a solution without calcium. This reaction occurs in a time-dependent manner. Additionally, peptide species between 25 and 30 kDa begin to emerge and an ~18 kDa fragment accumulates. When purified LeMCA1 was incubated with various pH buffers (pH 5.5–9.5) together with 50 mM Ca^{2+} for 30 min, the full-length protein was completely disappeared when incubated in a buffer with a pH between 7 and 8 (Fig. 3B). At other pH values, LeMCA1 showed weak or no cleavage pattern on the gel. These results indicated that the Ca^{2+}-induced autoprocessing of LeMCA1 is pH-dependent.

Ca^{2+}-induced LeMCA1 autoprocessing concomitant with the reduction of zymogen and accumulation of the small peptides (See Fig. 3A). We therefore addressed the question of which above mentioned process affected GRR activity, the LeMCA1 was preincubated for 20 min with Ca^{2+} to form processed LeMCA1 before adding the Boc-GRR-MCA substrate. Fig. S4 shows that preincubation with Ca^{2+} for 20 min caused the GRR activity to be reduced by 70% when compared with that not preincubation with Ca^{2+}. This result indicated that Ca^{2+}-inducing the reduction of the full-length protein seemed to contribute more for the activation of LeMCA1. Watanabe and Lam also showed the similar result of AtMC4, that the processed forms of AtMC4 at the later stage of Ca^{2+} incubation were catalytically inactive [14].

3.4. Key residues for the autoprocessing and activation of LeMCA1

The finding that LeMCA1 exhibits autocatalytic self-processing suggests that particular residues and structural features will affect autoprocessing and activation. Recently, McLuskey et al. used crystallization trials to identify calcium binding sites of MCA2 and four highly conserved aspartic acid residues: D173, D189, D190 and D220 were defined as calcium-binding sites [17]. Based on homology analysis, we predicted that D103, E104, D116 and D117 may represent the Ca^{2+} ligating residues of LeMCA1. In combination with our N-terminal sequencing results and other plant metacaspase identified cleavage sites and conserved catalytic sites, we construct five mutants: $LeMCA1^{C139A}$, $LeMCA1^{R186A/K269A}$, $LeMCA1^{K223G}$, $LeMCA1^{R332A}$ and $LeMCA1^{D116A/D117A}$ to identify key residues crucial for the activation and/or autoprocessing of tomato metacaspase.

After induction by IPTG and Ni-column purification, we first measure the GRR activities of the five mutants and compared the GRR activities with that of LeMCA1. Fig. 4A shows that mutations at the conserved catalytic site (C139A), N-sequenced cleaved sites (K223G and R332A) and the predicted Ca^{2+} binding sites (D116A/D117A) caused abrogation of GRR activity. Whereas mutation at both R186 and K269 (predicted autolysis sites) leaded to 60% reduction of GRR activity. AGPR-MCA, GKR-MCA and QKK-MCA substrates with Arg or Lys residue at the P1 position were used to measure the activities of the mutants that fail to cleave GRR substrate, and no fluorogenic signal was detected, whereas $LeMCA1^{R186A/K269A}$ displayed decreased activities compared with LeMCA1 when using different substrates (data not shown).

To further analyze the effects of the mutants on self-processing patterns, purified protein was analyzed by Western blotting. Fig. 4B showed that mutation at C139 or K223 gave rise to no cleavage. However, the Ca^{2+} binding site (D116A/D117A) mutant, cleaved site (R332) mutant and $LeMCA1^{R186A/K269A}$ double mutant

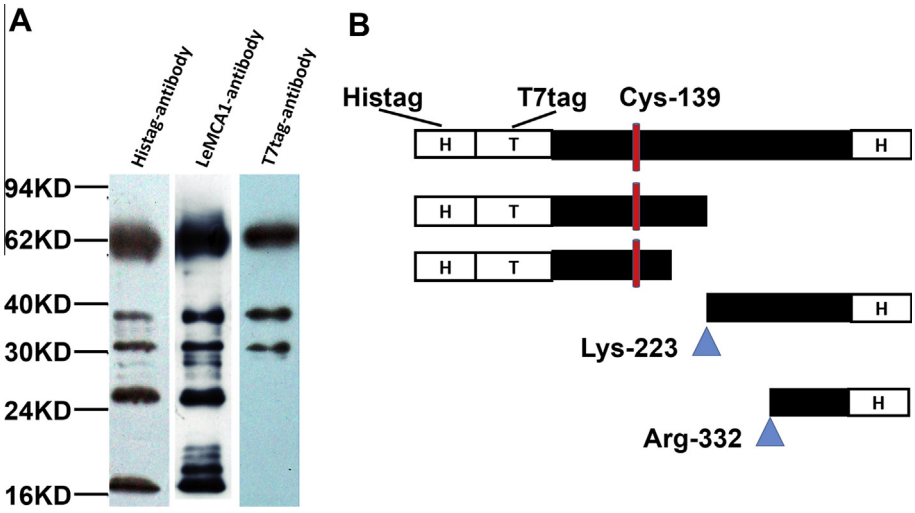

Fig. 2. Analysis of autoprocessing pattern of purified recombinant LeMCA1. (A) Immunoblot analysis of purified LeMCA1 using His tag-antibody LeMCA1-antibody, and T7 tag-antibody. (B) Schematic representation of self-processing sites in the LeMCA1 proteins determined by N-terminal protein sequencing. Construct map of LeMCA1 contains both N- and C-His tag, whereas T7 tag is in the N- termini. N-terminal sequencing confirmed cleaved sites represented by triangle. Catalytic Cys-139 also is marked in the map.

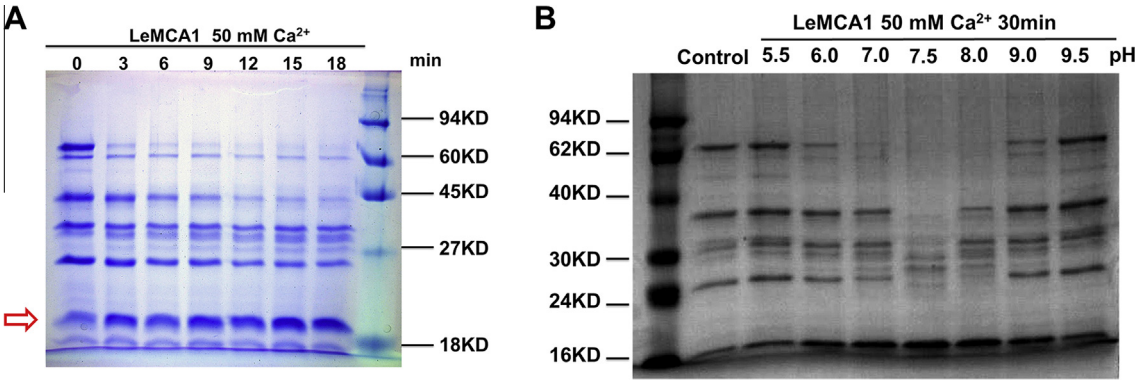

Fig. 3. Autoprocessing of LeMCA1 is Ca^{2+} and pH dependent. (A) Purified LeMCA1 were incubating with 50 mM Ca^{2+} for indicated time at room temperature, then separated in 12% SDS–PAGE. (B) LeMCA1 were preincubated with 50 mM Ca^{2+} for 30 min at different buffers (pH 5.5–9.5) as described under "Section 2", then analysis by SDS–PAGE. Control represents the LeMCA1 incubates without Ca^{2+} at pH 7.5 for 30 min.

still showed several bands following purification, indicating proteolysis still occurred when they expressed in bacteria. Interestingly, LeMCA1^{R332A} performed largely different protein signature compared with that of LeMCA1, in which the ~18 kDa processed form was absent as we predicted, and strangely formed two new bands around ~32 kDa (see Fig. 4B). For LeMCA1$^{D116A/D117A}$, in addition to lacking the ~36 kDa band, a fragment between ~32 and~26 kDa emerged, indicating Ca^{2+} binding sites seems likely in some extent altered the cleavage process of LeMCA1. Whereas LeMCA1$^{R186A/K269A}$ mutant caused the intensity of ~32 kDa fragment dropped significantly, which most likely representing the p20-like equivalent. This may be consistent with its decrease in GRR activity. Combined the results of various mutants indicated that LeMCA1 GRR activity and processing characteristics depend on both catalytic center Cys139 and cleaved Lys223 residues, whereas Arg332 and Asp116/Asp117 are necessary for the GRR activity in vitro but are not critical for the initial activation of the latent protein activity of the zymogen.

To gain additional information on whether calcium influences these mutants autoprocessing pattern, mutants were incubated with 50 mM Ca^{2+} at pH 7.5 for 30 min and SDS–PAGE analysis performed. Mutants C139, K223, R332 and D116/D117 showed no further cleavage after Ca^{2+} incubation. The full-length protein is stable and no obvious new bands appear (Fig. S5A–D). The R186/K269 mutant has a similar Ca^{2+}-dependent hydrolysis pattern to LeMCA1 (Fig. 5SE).

Taken together, Ca^{2+}-dependent full length zymogen cleavage seemed crucial for tomato LeMCA1 GRR activity. Catalytic C139, cleaved K223, R332 and our predicted calcium binding sites D116 and D117 represent key residues that are responsible for the full length protein cleavage by Ca^{2+} and the activation of LeMCA1 in vitro.

3.4.1. 3D structure prediction of LeMCA1 based on homology modeling

To predict the 3D structure of LeMCA1, we selected four crystal structures, GSU0716, caspase 7, Yca1 and MCA2, for LeMCA1 homology modeling using the Fold Prediction Algorithms. According to the structure evaluation, GSU0716 is the best scoring template which shares a sequence identity of 14.4% and has a 2.51 C-score. Only 3.5% of the residues lie outside the Ramachandran allowable range.

Fig. 5A shows the predicted 3D structure of LeMCA1 and its key residues location. Highly conserved residues Asp-103, Asp-116 and Asp-117 are in a concave area, folding together to form the spatial putative ion-binding area which is close to catalytic Cys-139, indicating that it may have an impact on the calcium-dependent

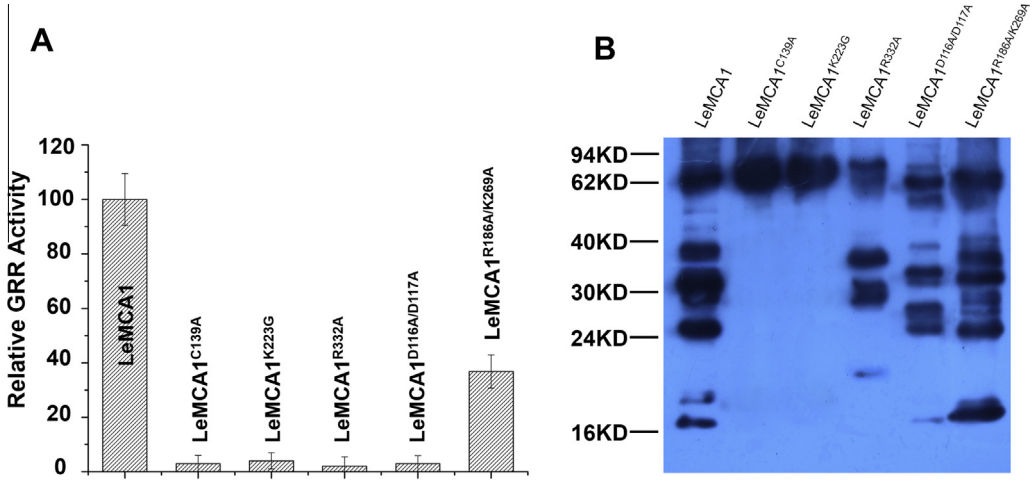

Fig. 4. GRR activities and autoprocessing patterns of key residues mutants. (A) GRR activities of LeMCA1 and five mutants. (B) Immunoblot analysis autoprocessing patterns of LeMCA1 and five mutants with anti-LeMCA1 antibody.

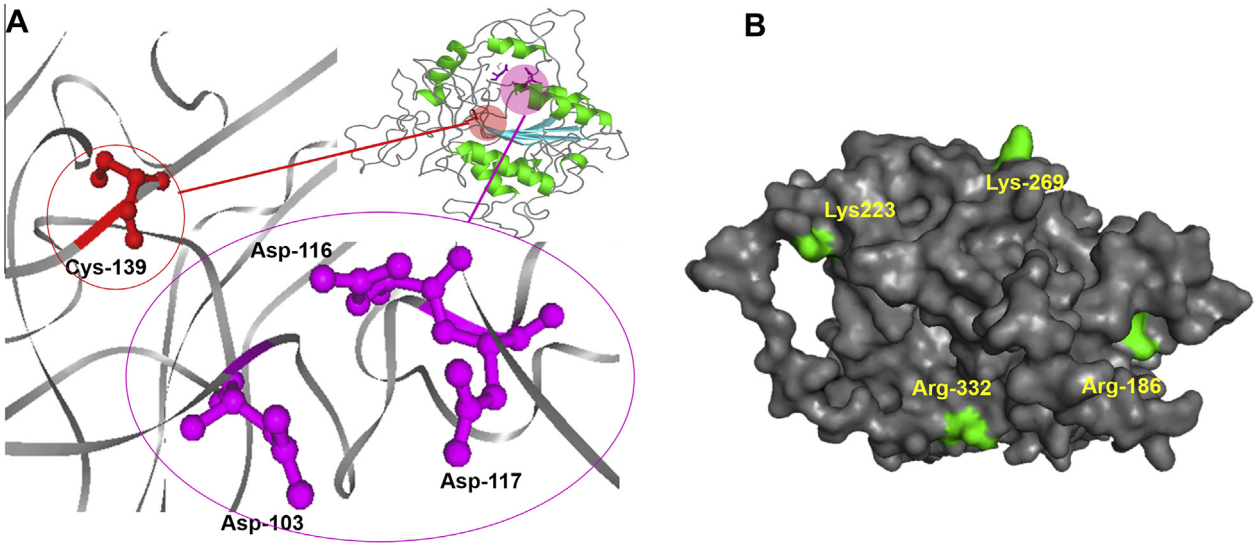

Fig. 5. 3D structure model of LeMCA1 constructed by homology modeling based on the crystal structure of protein GSU0716 in *Geobacter sulfurreducens* (3BIJ). (A) Ribbon diagram of LeMCA1 at top right corner, catalytic region was labeled by red color and calcium-binding area which was colored by pink. Close-up view of the key residues in two regions were circled. (B) Four cleaved sites Arg186, Lys223, Lys269 and Arg332 locate at the surface of LeMCA1.

activation of LeMCA1. In contrast, all the four cleavage sites locate at the surface of protein as is shown in Fig. 5B, suggesting that they may play roles in the pro-pro reaction or dimers forming as caspase. However, further detailed data from crystal and calcium bindings assays will provide more direct evidences.

4. Discussion

Processing is a typical characteristic for both caspases and metacaspases when they are overproduction in bacteria [15,18]. Our N-terminal sequencing results confirmed that recombinant tomato LeMCA1 catalytically cleaved at K223 and R332. In higher plants, only Arabidopsis AtMC9 and AtMC4 have confirmed autolysis sites at R183 and K225, respectively [14,15]. K223, K225 and R183 are highly conserved sites located at the linker region of type II metacaspase family (Fig. 2S), indicating autocleaved sites are likely to be conserved lysine or arginine residues among all plant type II metacaspase. However, no similar sites have been identified in type I metacaspase due to the lack of the linker region. Further, we showed that mutated LeMCA1 at K223 completely abrogated autolysis and activation even when the enzyme was incubated with Ca^{2+}. This finding is consistent with Watanabe's results of AtMC4, that the purified K225G form did not contain significant cleaved or self-processed forms [14]. However, the other cleaved site R332 is not conserved in plant metacaspase and locates near the C-terminal conserved group GIL(I/V)SGCQT of plant MCPs (Fig. S2). LeMCA1^{R332A} altered the processing pattern of the purified protein and also blocked the Ca^{2+} -induced the activation of LeMCA1 in vitro. Very interestingly, mutant at R332 also caused the disappearance of cleaved K223 (~26 kDa) band, suggesting that the processed R332 form would be a regulator involved in the cleavage of LeMCA1 at K223. Further investigations are needed to determine how R332 affect the cleavage at K223.

Additionally, substitution of the predicted calcium-binding residues, Asp116/Asp117, with alanine abrogated activity and the zymogen showed no obvious cleavage even after incubation with 50 mM Ca^{2+} for 30 min (Fig. S6). It seems likely that D116/D117 residues are essential for the Ca^{2+}-induced activation and zymogen processing of LeMCA1 in our in vitro reaction system. Similar to the Ca^{2+}-binding D189/D190 residues of MCA2, D116/D117 would be

involved in the Ca^{2+}-induced conformational shift of 280-like-loop to stabilize the interaction of active site and substrate [17]. In addition, this mutation did not prevent the autoprocessing when overexpressed in bacteria, which is inconsistent with the result of MCA2 Ca^{2+}-binding D189A/D190A mutant that did not processing [17]. It seems that LeMCA1 mutated at D116/D117 failed to inhibit cleavage at K223 and R332, but altered the sequential cleavage step or pattern of zymogen, which caused the incompletely maturation of LeMCA1. Although calcium binding regions are conserved in metacaspases from a diverse range of organisms, understanding the mechanism of calcium binding sites on autoprocessing still requires a large set of data from a variety of plant species.

Caspases, such as caspase-7, are activated by cleavage in the intersubunit linker generating the p10 and p20 subunits [18]. In plants, Bozhkov et al. [9] considered that R188 and K269 are two potential cleavage sites of Norway spruce mcII-Pa, which generate the p20 and p10 subunits; however, the importance of the predicted sites in enzyme activity has not been investigated. Based on sequence alignment, tomato LeMCA1 has conserved processing sites, R186 and K269. However, the LeMCA1$^{R186A/K269A}$ mutant retained autolysis ability to cleave full-length proteins in the presence of Ca^{2+} and showed ~40% GRR activity when compared with native LeMCA1. These results are similar with that of the Arabidopsis AtMC4$^{R190G/K271G}$ mutant, in which R190 and K271 were not required for AtMC4 activation [14]. Higher dicotyledon may be show more complex mechanism in the formation of subunits.

In summary, our data indicated that C139, K223, R332 and D116/D117 represent key residues for activation and autoprocessing of LeMCA1 in vitro. These data alone have not confirmed the order of autoprocessing and how Ca^{2+}, predicted Ca^{2+} binding residues regulate the cleavage of LeMCA1. Further investigation to find out active processed fragments of LeMCA1 and their regulation on the stress-induced plant cells death is necessary.

Acknowledgments

This work was supported by the National Basic Research Program of China (973 Program, Grant No.: 2013XB127104), the Modern Agroindustry Technology Research System (Grant No. ycytx-30-zy-05) and 863 Program (Grant No. 2012AA101702-2).

Appendix A. Supplementary data

Supplementary data associated with this article can be found, in the online version, at http://dx.doi.org/10.1016/j.febslet.2013.06.057.

Reference

[1] Rawlings, N.D., Barrett, A.J. and Bateman, A. (2010) MEROPS: the peptidase database. Nucleic Acids Res. 38, D227–33.
[2] Uren, A.G., O'Rourke, K., Aravind, L., Pisabarro, M.T., Seshagiri, S., Koonin, E.V. and Dixit, V.M. (2000) Identification of paracaspases and metacaspases: two ancient families of caspase-like proteins, one of which plays a key role in MALT lymphoma. Mol. Cell 6, 961–967.
[3] Tsiatsiani, L., Van Breusegem, F., Gallois, P., Zavialov, A., Lam, E. and Bozhkov, P.V. (2011) Metacaspases. Cell Death Differ. 18, 1279–1288.
[4] Ahmad, R., Zuily-Fodil, Y., Passaquet, C., Bethenod, O., Roche, R. and Repellin, A. (2012) Ozone and aging up-regulate type II metacaspase gene expression and global metacaspase activity in the leaves of field-grown maize (*Zea mays* L.) plants. Chemosphere 87, 789–795.
[5] Watanabe, N. and Lam, E. (2011) Arabidopsis metacaspase 2d is a positive mediator of cell death induced during biotic and abiotic stresses. Plant J. 66, 969–982.
[6] Wang, X.D., Wang, X.J., Feng, H., Tang, C.L., Bai, P.F., Wei, G.R., Huang, L.L. and Kang, Z.S. (2012) TaMCA4, a novel wheat metacaspase gene functions in programmed cell death induced by the fungal pathogen *Puccinia striiformis* f. sp. *tritici*. Mol. Plant Microbe Interact. 25, 755–764.
[7] Hoeberichts, F., Have, A. and Woltering, E. (2003) A tomato metacaspase gene is upregulated during programmed cell death in *Botrytis cinerea*-infected leaves. Planta 217, 517–522.
[8] He, R., Drury, G.E., Rotari, V.I., Gordon, A., Willer, M., Farzaneh, T., Woltering, E.J. and Gallois, P. (2008) Metacaspase-8 modulates programmed cell death induced by ultraviolet light and H_2O_2 in Arabidopsis. J. Biol. Chem. 283, 774–783.
[9] Bozhkov, P.V., Suarez, M.F., Filonova, L.H., Daniel, G., Zamyatnin, A.A., Rodriguez-Nieto, S., Zhivotovsky, B. and Smertenko, A. (2005) Cysteine protease mcll-Pa executes programmed cell death during plant embryogenesis. Proc. Natl. Acad. Sci. U. S. A. 102, 14463–14468.
[10] Lee, R.E.C., Brunette, S., Puente, L.G. and Megeney, L.A. (2010) Metacaspase Yca1 is required for clearance of insoluble protein aggregates. Proc. Natl. Acad. Sci. U. S. A. 107, 13348–13353.
[11] Richie, D.L., Miley, M.D., Bhabhra, R., Robson, G.D., Rhodes, J.C. and Askew, D.S. (2006) The *Aspergillus fumigatus* metacaspases CasA and CasB facilitate growth under conditions of endoplasmic reticulum stress. Mol. Microbiol. 63, 591–604.
[12] Ambit, A., Fasel, N., Coombs, G. and Mottram, J. (2007) An essential role for the *Leishmania* major metacaspase in cell cycle progression. Cell Death Differ. 15, 113–122.
[13] Moss, C.X., Westrop, G.D., Juliano, L., Coombs, G.H. and Mottram, J.C. (2007) Metacaspase 2 of *Trypanosoma brucei* is a calcium-dependent cysteine peptidase active without processing. FEBS Lett. 581, 5635–5639.
[14] Watanabe, N. and Lam, E. (2011) Calcium-dependent activation and autolysis of arabidopsis metacaspase 2d. J. Biol. Chem. 286, 10027–10040.
[15] Vercammen, D., van de Cotte, B., De Jaeger, G., Eeckhout, D., Casteels, P., Vandepoele, K., Vandenberghe, I., Van Beeumen, J., Inze′, D. and Van Breusegem, F. (2004) Type II metacaspases Atmc4 and Atmc9 of *Arabidopsis thaliana* cleave substrates after arginine and lysine. J. Biol. Chem. 279, 45329–45336.
[16] Giovannoni, J. (2001) Molecular biology of fruit maturation and ripening. Anu. Rev. Plant Biol. 52, 725–749.
[17] McLuskey, K., Rudolf, J., Proto, W.R., Isaacs, N.W., Coombs, G.H., Moss, C.X. and Mottram, J.C. (2012) Crystal structure of a *Trypanosoma brucei* metacaspase. Proc. Natl. Acad. Sci. U. S. A. 109, 7469–7474.
[18] Pop, C., Salvesen, G.S., Pop, C. and Salvesen, G.S. (2009) Human caspases: activation, specificity, and regulation. J. Biol. Chem. 284, 21777–21781.